# EXPERIMENTAL VALIDATION OF AN X-BAND ACTIVE ANTENNA FOR DATA DOWNLINK APPLICATIONS

Nelson J. G. Fonseca <sup>(1)</sup>, Bintou Doumbia <sup>(1)</sup>, Manon Bruneau <sup>(2)</sup>, Adrien Laffont <sup>(2)</sup>, Maxime Romier <sup>(1)</sup>, Nicolas Capet <sup>(1)</sup>

(1) ANYWAVES Toulouse, France Email: n.fonseca@anywaves.com

(2) ANYFIELDS Toulouse, France Email: adrien.laffont@anyfields.eu

Abstract—Future space missions with high-resolution microwave and optical instruments will require more sophisticated data downlink antennas. Anywaves has defined a roadmap to make commercially available an X-band payload data transfer phased array antenna capable of electronic beam steering compatible with typical low Earth orbit small satellite requirements.

A key aspect in the development of such a complex product is its validation and acceptance test sequence. While an extensive RF characterization is expected as part of the nominal development, time-efficient validation techniques are required in the production line. This paper explores alternative experimental validation techniques using a partial phased array demonstrator developed in the frame of a recent R&T activity supported by CNES. The preliminary results reported here are considered promising. The following steps will address the automation of a complete acceptance test sequence.

# I. INTRODUCTION

Payload data transfer (PDT) is a critical function of any scientific and Earth observation mission [1]. While smaller platforms (e.g., CubeSats and NanoSats) with limited processed data to offload may use the telemetry, tracking and command (TT&C) sub-system [2] for data downlink purposes, most satellites require a dedicated PDT sub-system. Various antenna solutions are available for data downlink [3], ranging from small fixed beam antennas [4] to more advanced radio frequency (RF) equipments, including for example a mechanically-steered beam pointing functionality [5].

Electronically-steered active antennas are emerging as a solution for future data downlink sub-systems onboard low Earth orbit (LEO) satellites, addressing the demanding requirements of upcoming high-resolution microwave and optical instruments [6]. With the support of CNES and industrial partners, Anywaves has defined

a roadmap to make commercially available an X-band antenna solution capable of steering its beam within a cone of 60° half-angle with reference to the antenna boresight. A first demonstrator was developed in the frame of an R&T activity aiming at validating the critical functions of the antenna [7]. A simplified version of the final product, with a one-axis scanning functionality to reduce the number of active control points, was designed, manufactured and tested.

A follow-up activity, aiming at the verification of a fully representative engineering model is on-going. In parallel, aspects related to the experimental validation and characterisation of such antennas are being investigated. There is a clear interest in exploring innovative ideas to provide an assessment of the good operation of the developed antenna within the short time frame often imposed on NewSpace developments. To this aim, two test campaigns were conducted, one using an MVG's Starlab, a spherical near-field setup, and another using the recently developed Anyfields' EMBox XL, an infrared thermography (IRT) solution.

This paper provides a high-level description of the envisioned PDT phased array antenna product. A partial demonstrator of this antenna was first tested in an anechoic chamber, using a far-field measurement setup. Alternative experimental validation techniques were also explored and are discussed in this contribution. The near-field measurements confirmed the good operation of the electronics, while the IRT helped identify some minor issues in the radiating panel.

### II. X-BAND PDT PHASED ARRAY ANTENNA

# A. Antenna System Architecture

Part of the spectrum in X-band is allocated to Earth Exploration Satellite Services (EESS). Specifically, the frequency band  $8.025 - 8.4\,\mathrm{GHz}$  is used for telemetry [2]. Additionally, the frequency band  $8.4 - 8.5\,\mathrm{GHz}$  is also available for space-to-Earth Space Research links. There is thus an interest in designing an antenna cover-

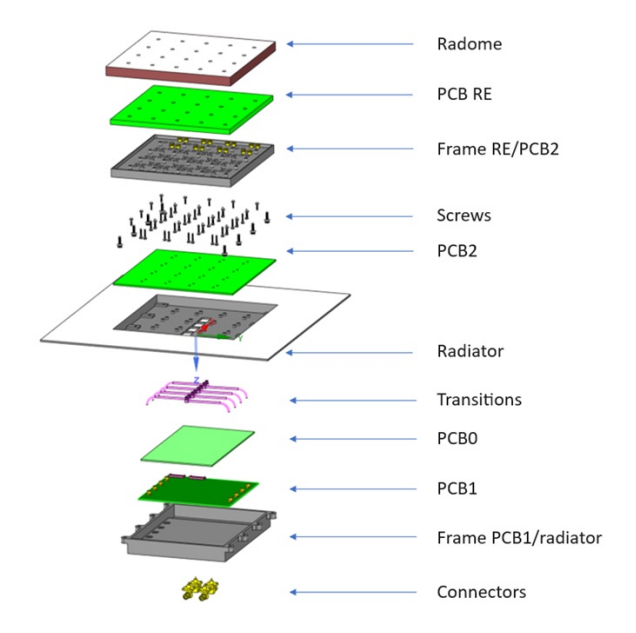


Fig. 1. Exploded CAD view of the X-band PDT phased array antenna product under development.

ing a wider frequency range from 8 to 8.5 GHz.

The targeted gain at the edge of coverage, i.e., at a scan angle of 60° from boresight compatible with most LEO mission requirements, is set to 20 dBi. This can be achieved with an  $8\times8$  patch antenna array solution. The objective of the antenna design is to have a parallel integration of all main printed circuit boards (PCBs), leading to a low-profile highly-integrated subsystem. An exploded CAD view of the X-band phased array product under development is provided in Fig. 1. The stack-up comprises a radiating element (RE) PCB, which integrates dual-polarized patch antenna elements in an hexagonal lattice, allowing a larger array spacing while preserving a grating-lobe free operation across the scan angle range considered. The array spacing is set to 17 mm, providing sufficient margins at the highest operating frequency specified.

The part PCB1 comprises a first beamforming stage, accounting for time delay between sub-arrays (the aperture is divided in four equal-sized sub-arrays) to reduce beam squint with frequency [8]. It is followed by PCB2, directly connected to the PCB RE, which comprises the main beamforming functionality produced with dedicated integrated circuits (ICs). Depending on the desired equivalent isotropic radiated power (EIRP), an external power amplifier may be required and integrated on PCB2. The complete antenna assembly has two connectors, as the antenna system is conceived to operate in two simultaneous orthogonal polarizations. Circular polarization is synthesized in PCB1, prior to the beamforming stage, since the two independent beams in orthogonal polarizations are expected to point in the same direction for data downlink applications.

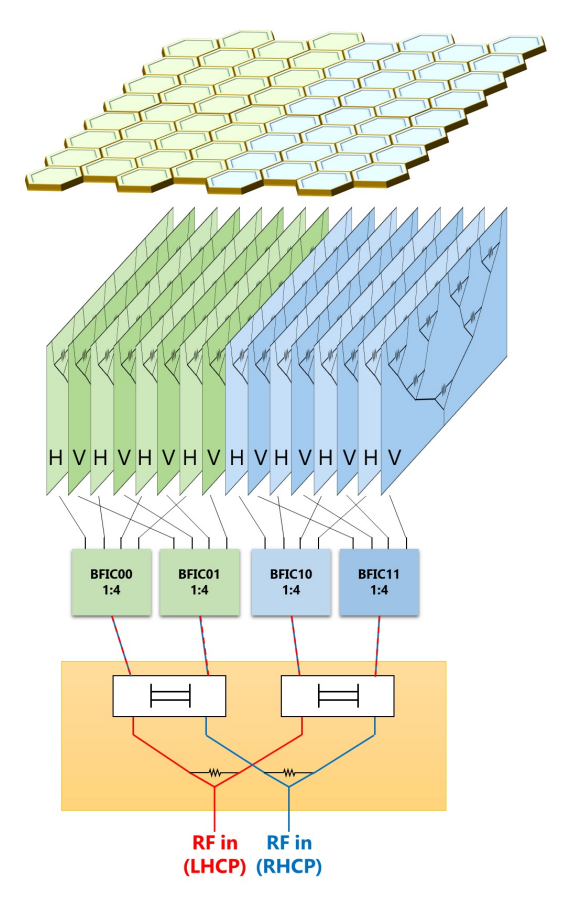


Fig. 2. Schematic view of the X-band PDT phased array antenna demonstrator with one-axis scanning functionality.

#### B. Demonstrator Definition and Testing

A first partial demonstrator of the envisioned phased array product was developed in the frame of a recently completed R&T study supported by CNES [7]. To simplify the overall design and focus on the critical functionalities to be evaluated with this proof-of-concept, a one-axis beam steering functionality was implemented, thus reducing the number of beamforming IC (BFIC) RF channels required. A simplified schematic view of the demonstrator, comprising the main constituting elements, is reported in Fig. 2. A total of 16 RF channels were necessary, addressing the two linear polarizations (H and V) of the 8 rows of elements. Power distribution along the orthogonal direction, per element row and per polarization, is achieved using passive beamforming networks. The BFICs implemented in this demonstrator are from Analog Devices Inc (ADI), with reference ADAR1000 [9]. The components in the yellow frame (i.e., the pairs of interconnected power dividers and directional couplers) in Fig. 2 represent the main functionalities embedded in PCB1, while the BFICs together with the passive beamformers correspond to the main functionality provided by PCB2 in Fig. 1.

The demonstrator is shown under test in an anechoic chamber in Fig. 3. The antenna is mounted on a posi-



Fig. 3. X-band PDT phased array antenna demonstrator under test in a far-field anechoic chamber setup.

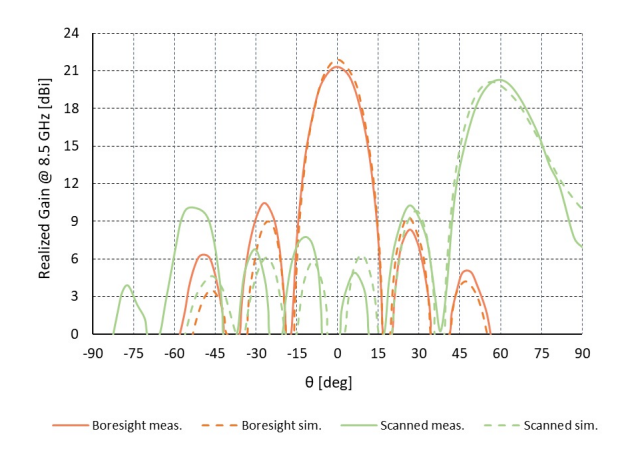


Fig. 4. Comparison of simulated and measured realized gain patterns (boresight and scanned beams) of the electronically-steered X-band PDT phased array antenna demonstrator.

tioner enabling mechanical scanning in the beamforming (horizontal) plane, thus providing the desired radiation pattern cuts. A sample of the results obtained is provided in Fig. 4. Excellent agreement is observed on the co-polarized radiated fields between simulated and measured results. The scanned beam achieves a realized gain greater than 20 dBi, as specified. The results are reported at 8.5 GHz, confirming the absence of grating lobes for the most scanned beam configuration at the highest operating frequency.

# III. EXPERIMENTAL VALIDATION

# A. Starlab Measurements

MVG's Starlab is a spherical near-field facility with a multi-probe circular arch enabling faster data acquisition [10]. The test facility available at Anywaves is a Starlab PRO operating from 650 MHz up to 18 GHz. The probe sampling angle is 22.5°. A complete sphere acquisition with the angular sampling necessary to process the data into far-field takes typically around 10 minutes, although this depends on the settings and specifically the speed of the actuators, which needs to

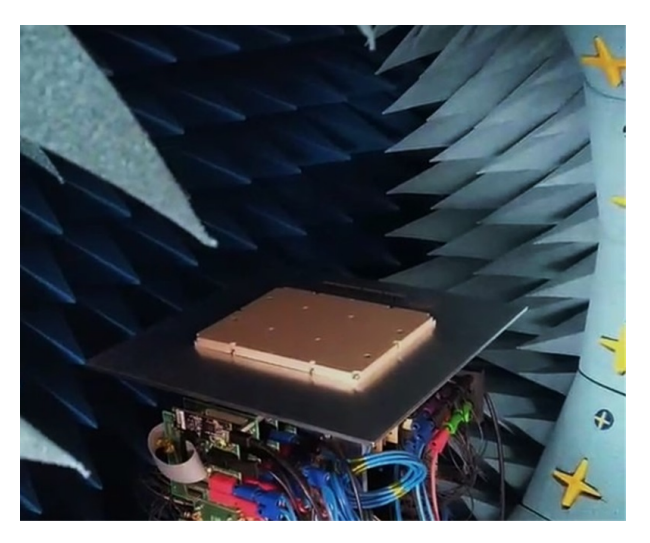


Fig. 5. X-band PDT phased array demonstrator under test in MVG's spherical near-field Starlab PRO facility.

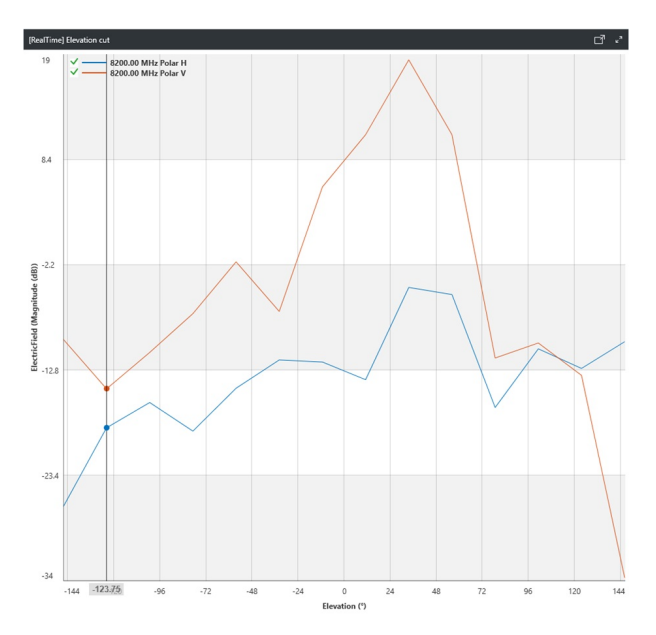


Fig. 6. Real time acquisition of the X-band PDT phased array beam pointing at  $30^{\circ}$  in MVG's spherical near-field Starlab PRO facility.

be set carefully considering the weight of the antenna under test (AUT). While this is substantially faster than conventional spherical near-field testing, this is typically longer than the time required to measure a single cut in far-field using the setup in Fig. 3.

The Starlab does provide an interesting feature in that it displays a real time acquisition of the data that can be monitored prior to launching a complete spherical near-field acquisition. This corresponds to a cut view of the radiative near-field produced by the antenna, as illustrated in Fig. 6 for a beam pointing at 30°. While the beam is not fully formed and the sampling is quite coarse, this still provides a time-efficient validation of

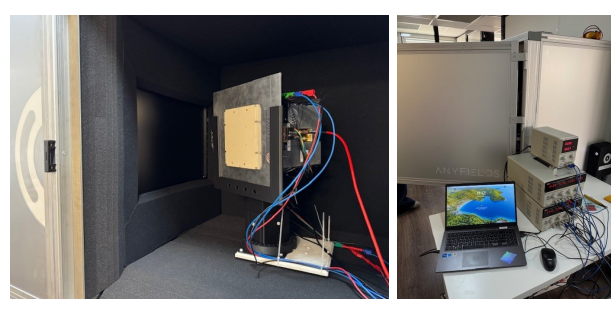


Fig. 7. X-band PDT phased array antenna demonstrator under test in Anyfields' EMBox XL.

the good operation of the antenna and a qualitative monitoring of the radiated power levels, both in co- and cross-polarized fields. This real time monitoring could be used to validate the good operation of the produced phased array in a more exhaustive manner, not feasible with conventional measurement techniques.

# B. EMBox XL Measurements

Anyfields has recently developed a larger version of their EMBox product, called the EMBox XL [11]. This equipment is large enough to accommodate the X-band phased array demonstrator and enabled a first trial of characterization using their proprietary IRT solution [12]. The test setup combines a thermosensitive film and an infrared camera within a compact anechoic measurement environment. The AUT is mounted on a rail system that allows for the adjustment of the measurement distance, as shown on Fig. 7. The power supply units and the laptop with ADI's user interface are located outside of the anechoic box. A typical acquisition and image processing time is in the order of 15 seconds, significantly faster than an RF measurement.

The AUT was placed 1 mm away from the film, providing an evaluation of the power distribution in the aperture. The processed IRT heat map obtained with all RF channels on is reported in Fig. 8. The BFICs were configured to have all RF channels in-phase and with the same amplitude, corresponding to the boresight beam configuration. While the level varies across the array, which is primarily attributed to alignment errors (i.e., the film not being perfectly parallel to the aperture) and parasitic effects (e.g., heat dissipated by the surrounding ground plane and electronic boards behind the aperture), there is a clear deep in the top left side of the array.

This prompted to perform additional acquisitions with one RF channel on at a time for the two BFICs controlling the left side of the array, one per polarization. The results are reported in Fig. 9 and Fig. 10 for respectively the BFIC00 and the BFIC01 (see Fig. 2), with one RF channel switched on at a time. These results helped identify some radiating elements with interconnection issues. Specifically, in the case of the BFIC00, feeding the H-polarization ports of the left half of the array, one

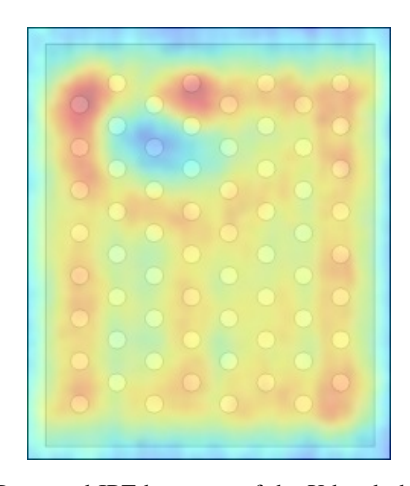


Fig. 8. Processed IRT heat map of the X-band phased array antenna demonstrator with all RF channels on.

element appears off (see Fig. 9), while with the BFIC01, feeding the V-polarization ports, at least two elements seem to be off. While these defects would be difficult to detect with synthesized patterns, as those reported in the previous section, owing to the very small number of faulty elements, this IRT method provides a more precise characterization of possible interconnection or PCB manufacturing issues. Investigations are on-going to understand the root cause of these defects.

While still preliminary, these results show the potential benefits of using IRT to validate the good operation of complex antennas and more specifically phased arrays in a time-efficient way. Combined with adequate signal processing techniques, it is anticipated that this method could provide a more exhaustive validation of a phased array antenna, supporting the early identification of potential defects as demonstrated here. Radiative near-field measurements, with the IRT film placed further away from the aperture, could also be envisaged to confirm the good synthesis of the desired patterns.

# IV. CONCLUSIONS

This paper provided an overview of the current activities at Anywaves to make commercially available an X-band phased array antenna solution compatible with typical requirements of small satellites in LEO. An important aspect of the work reported was the on-going activities to enable near real-time characterization of the antenna. Standard RF characterization techniques are not compatible with expected NewSpace production timelines. Aiming at a more exhaustive experimental validation of the hardware, two options have been investigated, one relying on the real-time data provided by MVG's Starlab spherical near-field and another using Anyfields' IRT approach. Both approaches may be complementary and further investigations are required to consolidate the conclusions of this work. The preliminary results reported here are considered promising.

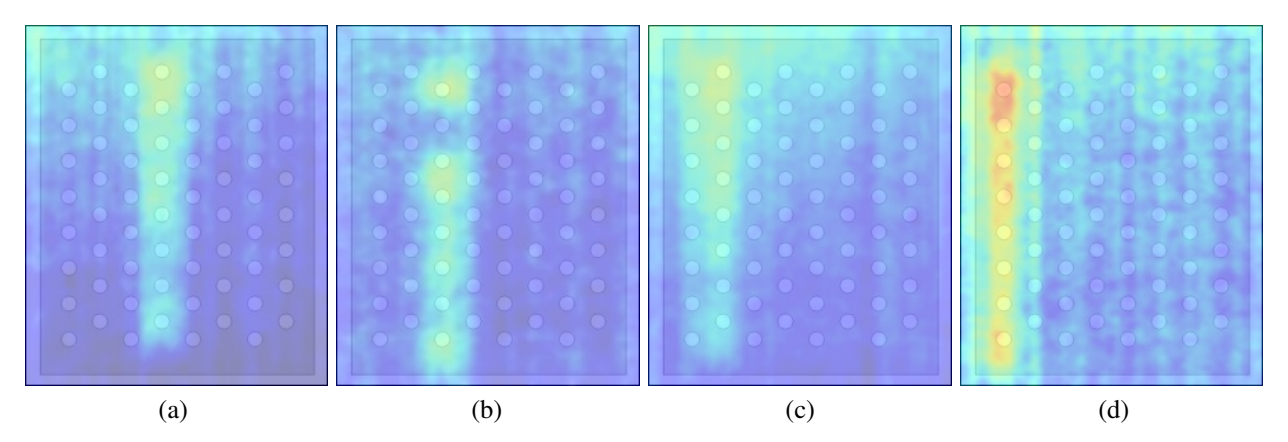


Fig. 9. Processed IRT heat map of the X-band phased array antenna demonstrator with the BFIC00 (a) Tx1, (b) Tx2 (c) Tx3 and (c) Tx4 RF channel on.

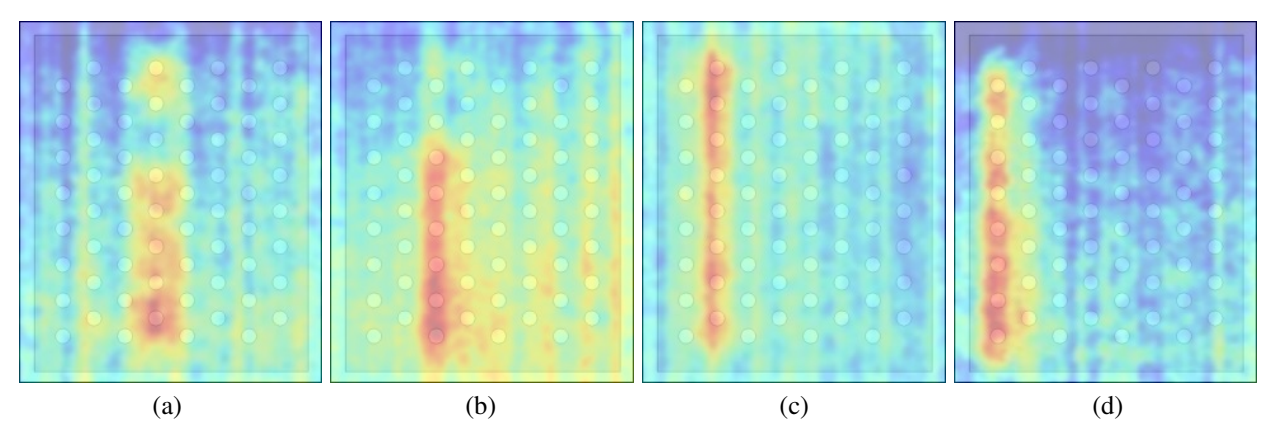


Fig. 10. Processed IRT heat map of the X-band phased array antenna demonstrator with the BFIC01 (a) Tx1, (b) Tx2 (c) Tx3 and (c) Tx4 RF channel on.

#### REFERENCES

- [1] https://www.esa.int/Enabling\_Support/Space\_ Engineering\_Technology/Radio\_Frequency\_Systems/ TT\_C\_and\_PDT\_Systems\_and\_Techniques\_section
- [2] A. Modenini and B. Ripani, "A Tutorial on the Tracking, Telemetry, and Command (TT&C) for Space Missions," *IEEE Commun. Surv. Tutor*, vol. 25, no. 3, pp. 1510-1542, 2023.
- [3] N. J. G. Fonseca, M. Romier, M. Del Mastro and N. Capet, "Data Downlink Antennas for Small Satellites in the NewSpace Era: Review and Perspectives," in *Proc. IEEE Int. Conf. WISEE*, Daytona, FL, USA, Dec. 2024.
- [4] B. Byrne, N. Capet and M. Romier, "Compact S-band and X-band antennas for CubeSats," CEAS Space J., vol. 12, pp. 587–596, 2020.
- [5] L. Bernabe, N. Raynal and Y. Michel, "3POD: A high performance parallel antenna pointing mechanism," in *Proc. ESMATS*, Noordwijk, The Netherlands, 2013.
- [6] N. Capet, N. J. G. Fonseca and M. Romier, "Innovative antenna solution for NewSpace: Addressing the challenges of small satellite constellations," in *Proc. Eur. Conf. An*tennas Propag. (EuCAP), Stockholm, Sweden, Apr. 2025.
- [7] J. Bhatker, M. Del Mastro, L. Mangenot and M. Romier, "Antenne a faisceau agile pour liens de telemesure charge

- utile en bande X," Seminaire COMET Antennes Actives, Toulouse, France, Apr. 2023.
- [8] N. J. G. Fonseca, A. Ali and H. Aubert, "Cancellation of Beam Squint with Frequency in Serial Beamforming Network-Fed Linear Array Antennas," *IEEE Antennas Propag. Mag.*, vol. 54, no. 1, pp. 32-39, Feb. 2012.
- [9] https://www.analog.com/en/products/adar1000.html
- [10] https://www.mvg-world.com/en/products/ antenna-measurement/multi-probe-systems/ the-new-starlab-portfolio
- [11] https://anyfields.eu/products
- [12] A. Laffont, S. Faure, M. Del Mastro, Q. Lamotte, J. Bhatker, M. Romier and D. Prost, "Near-field diagnosis of an X-band telemetry antenna using infrared thermography," in *Proc. Eur. Conf. Antennas Propag. (EuCAP)*, Florence, Italy, 2023.